

A Light-Weight Rotor Design for Brushless Doubly Fed Machines

Salman Abdi, Ehsan Abdi and Richard McMahon

Abstract – In this paper, a new optimized rotor design for Brushless Doubly Fed Machines (BDFMs) is proposed. The BDFM is considered as an attractive generator particularly for offshore wind power generation and also as a replacement for doubly fed slip ring induction generators. This is due to its higher reliability and lower maintenance reported in the literature. It is shown in this paper from the study of the magnetic field distribution in the rotor core that the conventional design of the BDFM rotor iron core can be modified, leading to a lighter machine. The proposed design method is supported by an analytical study and its practicality is validated using 2-D Finite Element (FE) analysis. A 250 kW experimental BDFM with frame size D400 is considered as the prototype machine.

Index Terms-- Brushless doubly fed machine (BDFM), rotor back iron, finite element analysis (FEA), magnetic circuit, iron saturation, magnetic flux density.

I. INTRODUCTION

THE Brushless Doubly Fed Machine (BDFM) is a variable speed generator or motor, which in recent years has been investigated as a possible replacement for the Doubly-Fed Induction Generator (DFIG) [1], currently used in majority of large wind turbines. Similar to the DFIG concept, a BDFM allows variable speed operation using a variable voltage, variable frequency (VVVF) converter rated at only a fraction (30-50%) of the generator rating [2], [3]. It also benefits from eliminating slip-rings and brush gear, thus reducing machine maintenance costs [4]. The BDFM also shares with the DFIG the ability to control the reactive power flow through the machine.

The BDFM is operated in its synchronous mode with one of its stator windings, called the power winding (PW), connected directly to the 3-phase grid and the second stator winding, called the control winding (CW) connected to a variable voltage variable frequency converter as shown in Fig. 1 [5], [6]. The number of poles for the stator windings are selected in a way to eliminate any direct coupling between the stator windings. The coupling is enabled through a specially-designed rotor winding [7].

To date, several large BDFMs have been manufactured, for instance in China with a 200 kW machine [8], in Brazil with the design of a 75 kW machine [9], and in the UK with the largest BDFM ever reported. The latter was designed, built and tested by the authors and some aspects of the

machine's performance were reported in [10] and [11]. The 250 kW BDFM is shown in Fig. 2, which was built in a frame size D400. However, to achieve successful large scale BDFMs for wind generation application with competitive economics and performance over the counterparts, it is essential to optimize the weight and size of the machine.

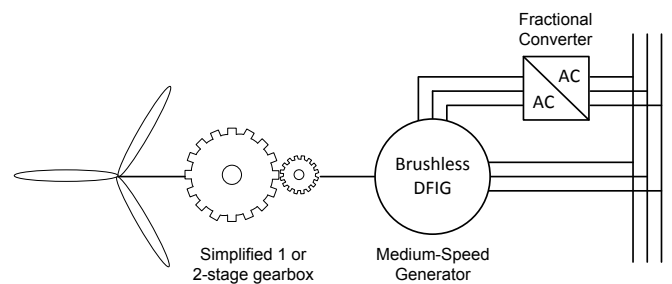


Fig. 1. A schematic of the wind turbine drive train with a BDFM as generator.



Fig. 2. D400 frame size BDFM (with red frame) and the load machine (with blue frame) on test rig.

Previous work on the analysis of the BDFM field distribution includes work by Creedy [12] and that by Williamson and Ferreira [13]. Creedy used a circle diagram or a time vector diagram to analyze the resultant rotor MMF distribution and found that the peak values of the rotor MMF are not equal at all angular positions and instead vary sinusoidally. He then used the observation to propose a design method for the BDFM rotor winding.

The observation made by Creedy regarding the peak values of the rotor field distribution was later reported by Liao et. al. [14] for the design of the BDFRM (Brushless

S. Abdi is with Faculty of Engineering, Environment and Computing, Coventry University, Coventry, UK (e-mail: ac7019@coventry.ac.uk).

E. Abdi is with Wind Technologies Ltd, Cambridge, UK (email: ehsan.abdi@windtechnologies.co.uk).

R. McMahon is with Warwick Manufacturing Group (WMG), University of Warwick, UK (email: r.mcmahon.1@warwick.ac.uk).

Doubly Fed Reluctance Machine). A BDFRM has two stator windings of different pole numbers similar to the BDFM, but uses a reluctance rotor to couple the stator winding fields.

Williamson and Ferreira [13] also investigated the BDFM field distribution by comparing plots of the flux density distribution across the cross-section of the machine using a time-stepping finite element model at consecutive time instances; an example is shown in Fig. 3. They reported from the comparison, that the movement of the field is not a matter of simple rotation and that it is far more complex. Also, that the field distribution does not have a clear n-pole pattern.

In this paper, an analytical study of the BDFM rotor field distribution is performed showing that the field distribution in the rotor magnetic circuit in a BDFM does not depend on the rotor speed. In addition, the peak flux density in different parts of the rotor iron including the back iron and rotor teeth sections alters with angular position. It can therefore be concluded that only certain parts of the rotor iron circuit experience high level of magnetic flux density independent of time and operating conditions.

Based on the analysis, a new light-weight rotor design is proposed in this paper by removing some parts of the rotor back iron, which do not effectively take part in the machine magnetic circuit. 2-D Finite Element (FE) models are then developed and analyzed for the prototype BDFM with the original and new design rotors being considered. The performance results from the new rotor design are compared to the original design.

II. PROTOTYPE MACHINE CONSIDERED IN THIS STUDY

Table I gives detailed information for the prototype machine used in this study. The machine stack length was 820 mm and both PW and CW stator windings were connected in delta. The rotor is a nested-loop design consisting 60 slots. As the prototype machine has $p_1 = 2$ and $p_2 = 4$, the rotor has $p_1 + p_2 = 6$ nests terminated with a common end ring at one end only [15]. Each nest is allocated 10 slots. Therefore, five concentric loops are housed within each nest [16]. The machine is shown in Fig. 2 on the experimental rig. The magnetization data for stator and rotor laminations were given by the manufacturer.

TABLE I
D400 BDFM DESIGN SPECIFICATIONS

Frame size	D400
PW pole-pair number	2
PW rated voltage	690V at 50Hz (delta)
PW rated current	178 A (line)
CW pole-pair number	4
CW rated voltage	620V at 18Hz (delta)
CW rated current	74 A (line)
Speed range	500 rpm \pm 33%
Rated torque	3700 Nm
Rated power	250 kW
Efficiency	> 96%
Stack length	820 mm

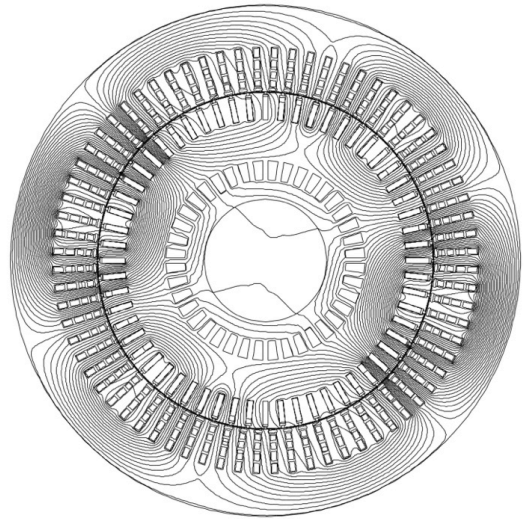


Fig. 3. D400 BDFM magnetic flux distribution in synchronous mode of operation obtained from 2-D Finite Element (FE) simulation.

III. ROTOR MAGNETIC CIRCUIT OPTIMIZATION

A. Variation of Peak Flux Density with Angular Position

Equation (1) represents the distribution of the BDFM magnetic field, generated by its rotor and stator windings for different stator supply frequencies of f_1 and f_2 [17]:

$$B(\theta, t) = \hat{B}_1 \cos(2\pi f_1 t - p_1 \theta) + \hat{B}_2 \cos(2\pi f_2 t - p_2 \theta + \alpha) \quad (1)$$

where:

- \hat{B}_1 and \hat{B}_2 are the values of peak flux densities for stator PW and CW, respectively, in T.
- f_1 and f_2 are the stator PW and CW excitation frequencies, respectively, in Hz.
- θ is the angular position and varies between $[0^\circ: 360^\circ)$
- α is the phase angle offset between PW and CW flux densities.

In (1) the effects of finite distributions of windings conductors, slotting effects and iron saturation are neglected. It should also be noted that the value of α determine the relative positions of the $2p_1$ and $2p_2$ pole flux density waveforms and can only be altered by changing the excitation phase angles of the stator windings since the physical positions of the windings are fixed. The field components in the rotor frame when the $2p_1$ -pole and $2p_1$ -pole field components rotate in the same direction relative to the rotor can be determined from (1) when

$$f_1 = f_2 \quad (2)$$

This is the preferred form of BDFM operation called 'Cumulative' mode of operation [18]. However, the stator excitation frequency values, f_1 and f_2 are related to the shaft speed (N) in *rpm* given by:

$$N = 60 \frac{f_1 \pm f_2}{p} \quad (3)$$

where p is either equal to $p_1 - p_2$ or $p_1 + p_2$ for the differential and cumulative BDFM, respectively. Therefore, the field distribution in the stator magnetic circuit depends on the

rotor speed and that of the rotor does not. For the case of $f_1 = f_2$, (1) can be expressed as the sum of traveling and standing waves.

$$B(\theta, t) = 2B_1 \cos\left(\frac{P_1 - P_2}{2}\theta\right) \times \cos\left(2\pi f_1 t - \frac{P_1 + P_2}{2}\theta\right) + (B_2 - B_1) \cos(2\pi f_1 t - p_2\theta) \quad (4)$$

In (4) the peak value of $B(\theta, t)$ is varied at different angular positions due to the standing wave term, i.e.:

$$B(\theta, t) = 2B_1 \cos\left(\frac{P_1 - P_2}{2}\theta\right) \times \cos\left(2\pi f_1 t - \frac{P_1 + P_2}{2}\theta\right) \quad (5)$$

As obvious, the amplitude of the standing wave term in (4) varies sinusoidally with θ . Therefore, it can be concluded that the distribution of the rotor field is independent of the rotor operating speed and, furthermore, the peak flux density in different parts of the rotor iron including different back iron and teeth sections varies with angular position as the absolute value of a sinusoidal wave. In the next section a time-stepping finite element analysis of the BDFM rotor field distribution is performed in order to further investigate the analytical results.

B. Finite Element Analysis of Rotor Field Distribution

The experimental D400 BDFM is simulated in finite element (FE) simulation software in its synchronous mode of operation, taking the iron and magnetic wedges nonlinear properties into account. The magnetic wedges have been used in stator slot openings in order to lessen the required magnetizing currents in stator windings. The rotor configuration is a nested-loop design with six nest and five loops per nest. It was proved in [19] that the BDFM has 180° symmetry in its magnetic flux pattern and therefore only half of the machine cross-section is simulated, which reduces the computational time significantly.

The rotor mesh for a single nest span i.e. 60° is shown in Fig. 4. The rotor back iron mesh elements are depicted in different colours, where, the elements with the same colour have the same distance from the rotor centre. Fig. 5 shows the peak flux density values for the elements located at each colour group obtained from FE post processing. As can be seen, the peak flux density in rotor back iron is lowest and highest between two adjacent nests and in the centre of each nest, respectively. In addition, the variation of the peak flux density for the regions nearer to the rotor shaft is much higher and therefore, larger iron parts can be removed from the region closer to the shaft.

C. A New Design For the BDFM Rotor Back Iron

Based on the above analysis of the rotor flux distribution, a new rotor back iron design has been proposed. Fig. 6 shows the cross section of the new design for the D400 BDFM rotor. It should be noted that the two regions specified inside the dashed circle as A and B do not take active part in the magnetic circuit, and hence their design is mainly determined by mechanical and cooling restrictions such as the rotor iron losses and the minimum required stiffness of region A. The analysis of mechanical and cooling requirements are outside the scope of this paper.

However, the rotor back iron outside the dashed line contributes to the rotor magnetic circuit and hence its design affects the machine performance. In the new design method as shown in Fig. 6, the regions further from nest centre have thinner back iron depth since they experience lower peak flux density. In addition, the rotor back iron regions closer to the nest centres require thicker iron since experiencing higher magnetic peak flux density. These design considerations agree

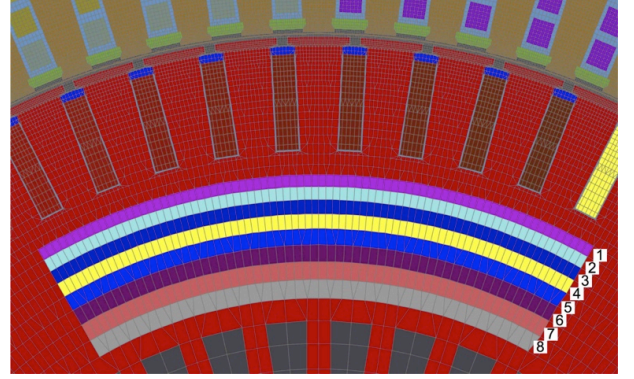


Fig. 4. A view of the rotor back iron mesh for a single nest span; The elements with different distance from the centre are shown with different colours.

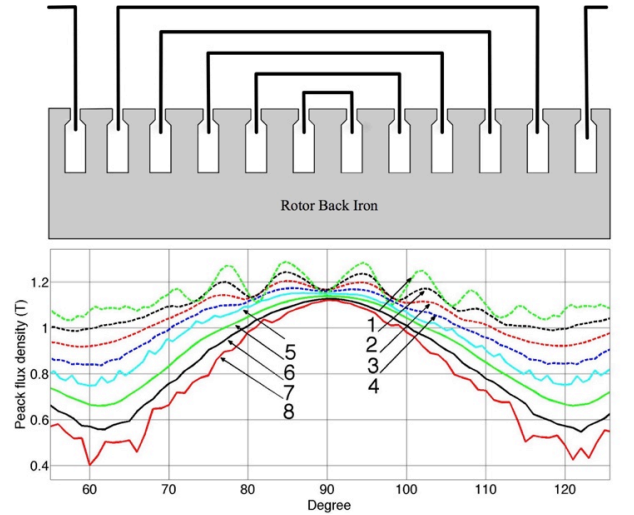


Fig. 5. The rotor peak flux densities for the back iron elements of a single nest span. The numbers specified to plots of this figure are corresponding to the numbers in Fig. 4.

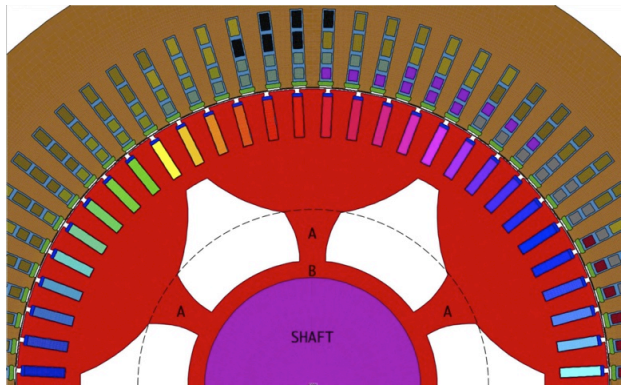


Fig. 6. The new light-weight rotor design.

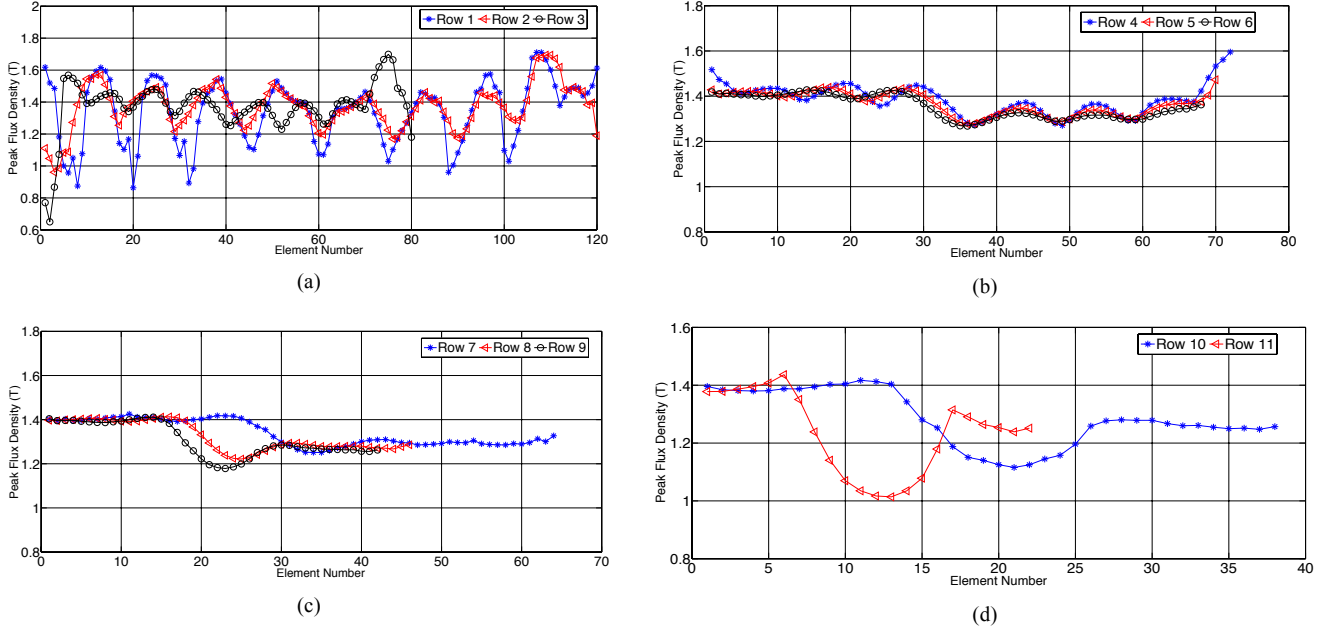


Fig. 8. The values of peak flux density in the rotor back iron elements shown in Fig. 7. (a) Rows 1, 2, and 3. (b) Rows 4, 5, and 6. (c) Rows 7, 8, and 9. (d) Rows 10 and 11

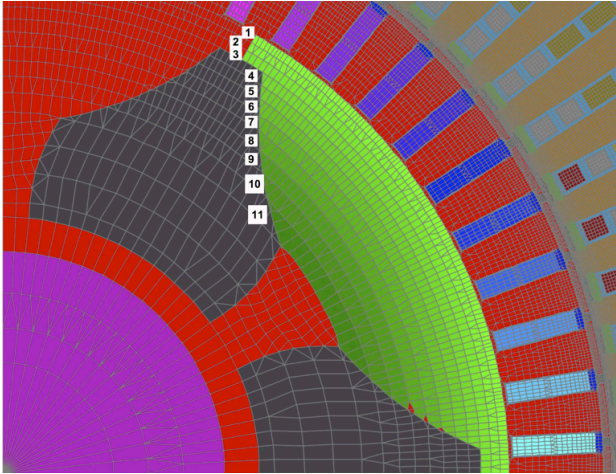


Fig. 7. Rotor back iron elements between two chunks of the new designed rotor. Elements on different rows have been specified with different colours.

TABLE II
D400 BDFM OPERATING CONDITIONS IN SYNCHRONOUS MODE OF OPERATION

Frame Size	D400
Speed (rev/min)	650
Torque (Nm)	3600
$ V_{4-pole} $ (V)	690
f_{4-pole} (Hz)	50
$ V_{8-pole} $ (V)	606
f_{8-pole} (Hz)	15

with what is proved analytically in Section A and also observed in FE simulations of the rotor flux distribution.

The weight optimisation procedure includes removing some chunks from the rotor back iron where the magnetic fields are weaker i.e. the areas between nests, then checking the peak flux density values to ensure that they stay below within the acceptable range. The procedure may continue until the peak flux densities reach the design targets for the rotor back iron.

After applying the weight optimisation procedure to the rotor back iron, the performance and characteristics of D400 BDFM with the new designed rotor is assessed in the synchronous operating mode.

The BDFM operating conditions are given in Table II. The machine was supplied with rated stator PW and CW voltages and no noticeable increase was observed in the values of stator windings currents and machine torque when the new rotor back iron design is used. In addition, in order to assess the rotor back iron saturation in the new design, the peak flux density values for the elements shown in Fig. 7 in green, are plotted in Fig. 8. As can be observed, the peak flux densities in all elements are below $1.8 T$, which is within the design limit.

The magnetic flux lines and the flux density modulus when the BDFM is run in its synchronous mode are shown in Fig. 9. The supplied voltages and frequencies have been kept at the rated values as given in Table II. As it can be seen, in the synchronous mode, which is the BDFM desirable mode of operation, and under rated conditions, no excessive saturation can be observed in machine magnetic circuit confirming the practicality of the new rotor back iron design method.

IV. CONCLUSIONS

In this paper a new design method has been proposed for the BDFM magnetic circuit, in order to reduce the rotor weight. BDFMs are attractive machines as generators for wind turbines and particularly as a replacement for doubly-fed induction generators. It is therefore essential to optimize the weight and size of the machine before a megawatt-scale BDFM is being built making it possible to use the BDFM in existing turbines.

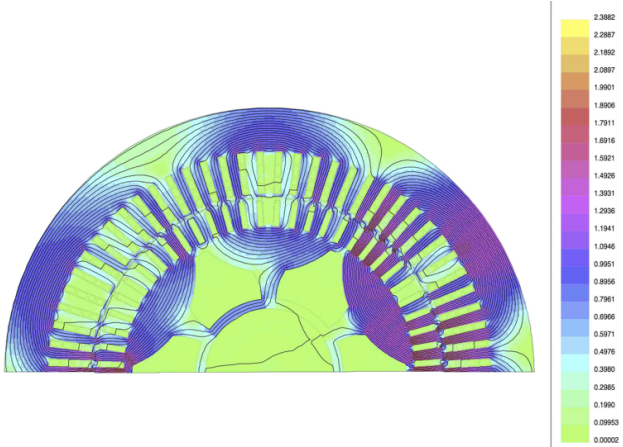


Fig. 9. The flux density magnitude colour for D400 BDFM in synchronous mode of operation, obtained from FE non-linear analysis

It has been shown that the rotor back iron peak flux density varies with angular position, independent of the shaft speed. It has consequently been shown that some parts of the rotor back iron do not take part in the machine magnetic circuit and therefore can be removed. This finding has been used to design a new light-weight rotor in which $p_1 + p_2$ chunks were removed. The FE simulations have validated the proposed design methodology. The proposed light-weight design has led to 21% reduction in the rotor's weight and 7.8% reduction in the machine's total weight for the D400 prototype BDFM.

V. REFERENCES

- [1] A. Wallace, R. Spee, and G. Alexander, "Adjustable speed drive and variable speed generation systems with reduced power converter requirements." *Budapest: ISIE IEEE international Symposium on Industrial Electronics*, June 1993, pp. 503 – 508.
- [2] C. S. Brune, R. Spee, and A. K. Wallace, "Experimental evaluation of a variable-speed, doubly-fed wind-power generation system," *IEEE Trans. Industry Applications*, vol. 30, no. 3, pp. 648 – 655, 1994.
- [3] R. A. McMahon, X. Wang, E. Abdi-Jalebi, P. J. Tavner, P. C. Roberts, and M. Jagiela, "The bdfm as a generator in wind turbines." *12th International Power Electronics and Motion Control Conference, EPE-PEMC*, September 2006.
- [4] E. Abdi, A. Oraee, S. Abdi, R. McMahon, "Design of the Brushless DFIG for Optimal Inverter Rating", *7th IET International Conference on Power Electronics, Machines and Drives (PEMD 2014)*.
- [5] S. Abdi, E. Abdi, R. McMahon, "A Study of Unbalanced Magnetic Pull in Brushless Doubly Fed Machines" *IEEE Trans. Energy Conversion*, DOI: 10.1109/TEC.2015.2394912, 2015.
- [6] R. A. McMahon, P. C. Roberts, X. Wang, and P. J. Tavner, "Performance of bdfm as generator and motor," *Electrical Power Applications, IEE Proceedings*, vol. 153, no. 2, pp. 289–299, March 2006.

- [7] S. Abdi, E. Abdi, A. Oraee, R. McMahon, "Investigation of magnetic wedge effects in large-scale BDFMs" *Renewable Power Generation Conference (RPG 2013)*, 2nd IET, pp. 1 – 4.
- [8] H. Liu and L. Xu, "Design and performance analysis of a doubly excited brushless machine for wind power generator application." *IEEE International Symposium on Power Electronics for Distributed Generation Systems*, 2010, pp. 597 – 601.
- [9] R. Carlson, H. Voltolini, F. Runcos, P. Kuo-Peng, and N. Baristela, "Performance analysis with power factor compensation of a 75 kw brushless doubly fed induction generator prototype." *IEEE International Conference on Electric Machines and Drives*, 2010.
- [10] E. Abdi, R. McMahon, P. Malliband, S. Shao, M. Mathekga, P. Tavner, S. Abdi, A. Oraee, T. Long, and M. Tatlow, "Performance analysis and testing of a 250 kw medium-speed brushless doubly fed induction generator," *Renewable Power Generation, IET*, vol. 7, no. 6, pp. 631 – 638, 2013.
- [11] S. Abdi, E. Abdi, A. Oraee, R. McMahon, "Equivalent Circuit Parameters for Large Brushless Doubly Fed Machines (BDFMs)" *IEEE Trans. Energy Conversion*, vol. 29, no. 3, pp. 706 – 715, 2014.
- [12] F. Creedy, "Some developments in multi-speed cascade induction motors," *Institute of Electrical Engineers Journal*, pp. 511–537, 1920.
- [13] S. Williamson and A. C. Ferreira, "Generalised theory of the brushless doubly-fed machine. Part 2: model verification and performance," *IEE Proceedings - Electric Power Applications*, vol. 144, no. 2, pp. 123–129, 1997.
- [14] Y. Liao, L. Xu, and L. Zheng, "Design of a doubly fed reluctance motor for adjustable speed drives," *IEEE Transactions on Industry Applications*, vol. 32, pp. 1195–1203, September/October 1996.
- [15] R. McMahon, P. Tavner, E. Abdi, P. Malliband, and D. Barker, "Characterising brushless doubly fed machine rotors," *IET Electric Power Applications*, vol. 7, pp. 535 – 543, 2013.
- [16] R. A. McMahon, E. Abdi, P. Malliband, S. Shao, M. E. Mathekga, and P. J. Tavner, "Design and testing of a 250 kw brushless dfig." Bristol, UK: *6th IET International Conference on Power Electronics, Machines and Drives (PEMD)*, March 2012.
- [17] S. Williamson, A. C. Ferreira, and A. K. Wallace, "Generalised theory of the brushless doubly-fed machine—Part 1: Analysis," *Proc. IEE Elect. Power Appl.*, vol. 144, pp. 111–122, 1997.
- [18] A. R. W. Broadway and L. Burbridge, "Self-cascaded machine: A low speed motor or high frequency brushless alternator," *Proc. IEE*, vol. 117, pp. 1277–1290, 1970.
- [19] A. M. Oliveira, P. Kuo-Peng, N. Sadowski, F. Runcos, R. Carlson, and P. Dular, "Finite-element analysis of a double-winding induction motor with a special rotor bars topology," *IEEE Transactions on Magnetics*, vol. 40, no. 2, pp. 770–773, March 2004.

VI. BIOGRAPHIES

Salman Abdi received the B.Sc. degree from Ferdowsi University, Mashhad, Iran, in 2009 and the M.Sc. degree from Sharif University of Technology, Tehran, Iran, in 2011, both in electrical engineering. He then received his Ph.D. degree in electrical machines design and modeling and instrumentation in July 2015 from Cambridge University, UK. He was appointed as a Research Associate in Cambridge University, Engineering Department in 2015, and then as a Research Fellow in Warwick Manufacturing Group (WMG), University of Warwick in 2016. He is currently a Lecturer in Electrical Engineering in the Faculty of Engineering, Environment and Computing, Coventry University, UK. His main research interests include electrical machines and drives for renewable power generation, Power Electronics and Control Systems.

Ehsan Abdi received the B.Sc. degree from Sharif University of Technology, Tehran, Iran, in 2002 and the M.Phil. and Ph.D. degrees from Cambridge University, Cambridge, U.K., in 2003 and 2006, respectively, all in electrical engineering. He is currently a Fellow of Churchill College, Cambridge University and the Managing Director of Wind Technologies Ltd. where he has been involved with commercial exploitation of the brushless doubly fed induction generator technology for wind power applications. His main research interests include electrical machines and drives, renewable power generation, and electrical measurements and instrumentation.

Richard McMahon received the B.A. degree in electrical sciences and the Ph.D. degree in electrical engineering from Cambridge University, Cambridge, U.K., in 1976 and 1980, respectively. Following postdoctoral work on semiconductor device processing, he was appointed as the University Lecturer in the Department of Electrical Engineering, Cambridge

University, in 1989, and became a Senior Lecturer in 2000. In 2016 he was appointed as the Head of Power Electronics group in Warwick Manufacturing Group (WMG), University of Warwick, and became a Professor. His research interests include electrical drives, power electronics, and semiconductor materials.